CONSTRUCTION OF A LOW-SPEED CLOSED-RETURN WIND TUNNEL

By

Jonathan G. Durbin

A thesis submitted in partial fulfillment of the requirements for the degree of

Bachelor of Science

Houghton College

May 11, 2019

Signature of Author……………………………………………………………………………………..

Department of Physics

May 11, 2019

……..

Dr. Kurt Aikens

Assistant Professor of Physics

Research Supervisor

……..

Dr. Mark Yuly

Professor of Physics

CONSTRUCTION OF A LOW-SPEED CLOSED-RETURN WIND TUNNEL

By

Jonathan G. Durbin

Submitted to the Department of Physics
on May 11, 2019 in partial fulfillment of the
requirement for the degree of
Bachelor of Science

Abstract

A small-scale, low-speed, closed-return wind tunnel is being designed and constructed at Houghton College to provide opportunities for further education and new research. Empirical correlations were used by previous researchers to generate a preliminary design based on various constraints. Examples of such constraints include the size of the room, the speed within the test section, and the desired flow quality. The wind tunnel will be 4.72 meters long, have an area ratio of 5.45 between the nozzle and test section, a maximum test section speed of 44.7 m/s (100 mph), and one side of the wind tunnel will be made almost entirely out of plexiglass. The wind tunnel will also have a maximum Reynolds number per meter of 3×10^6 (Reynolds number per foot of 9×10^5). In this thesis, specific attention is given to one of the diffusers and two of the corners. Additional details for the other components of the wind tunnel will be presented and future work discussed.

Thesis Supervisor: Dr. Kurt Aikens
Title: Assistant Professor of Physics

TABLE OF CONTENTS

TABLE OF FIGURES

Chapter 1

BACKGROUND AND MOTIVATION

1.1. History of Experimental Aerodynamics

Wind tunnels are a crucial instrument in gaining a better understanding of aerodynamics. They are used to better understand the physics of fluid flows and to measure how fluids act on objects as they move through them. Before wind tunnels became mainstream, researchers used other methods to conduct their fluid dynamics experiments. Much of the discussion in the next sections contains information from Ref. [1].

1.1.1. Before the Wind Tunnel

Some early experimenters such as Isaac Newton and Leonardo da Vinci knew that controlled environments were necessary to measure how an object would move through a fluid such as air. They knew that an object must either be moved through the air at a high velocity or have air moved over it at a high velocity while it is fixed. In the early days of experimental aerodynamics, tests would be conducted in areas where there was reliably strong wind, like caves and steep cliffs. This method was beneficial because it was inexpensive, and experiments could be conducted for long amounts of time. However, it quickly became clear that locations like these did not yield airflow that was uniform and steady enough such that measurements could be obtained with small uncertainties. Experimenters soon turned to mechanical means to move their models through still air in an effort to study a more controlled system.

The most common method was the whirling arm, as seen in Figure 1. Using the whirling arm, one could attach airfoils or other objects to measure forces such as lift and drag. To measure lift and drag, the object was first allowed to reach a constant speed [2]. Once there is no acceleration, the torque produced by drag perfectly counters the torque produced by the falling mass, allowing drag to be measured. The lift force was determined by attaching weight to the object as a counterbalance such that it remained horizontal at speed. A stopwatch was also used to time full revolutions of the object to determine its speed. The whirling arm method was helpful in establishing basic aerodynamic data, but it had its flaws. It was challenging to mount complex shapes to the end of the whirling arm and measure exactly the small forces present, especially at high speeds. Furthermore, objects mounted to the end of the whirling arm would fly into their own wake because the air surrounding the arm was “stirred” into rotational motion. Additionally, the object had to reach terminal velocity before measurements could be taken. These kinds of problems prompted the development of the wind tunnel.

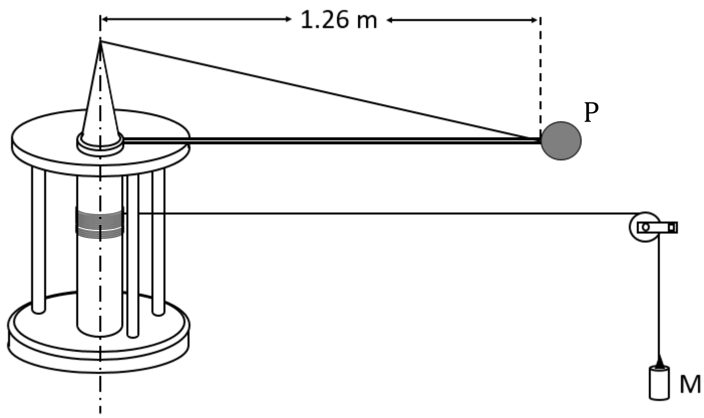

Figure 1. Diagram of a whirling arm. A mass M falls, causing a drum to spin, allowing the lift and drag of the attached object P to be measured using counter weights [2]. This whirling arm was used by the British mathematician Benjamin Robbins. In some variations of the whirling arm, a counter-balance is attached to support the weight of P. Figure adapted from Ref. [1].

1.1.2. The Wind Tunnel

A wind tunnel is an experimental aerodynamics apparatus used to measure the impacts of fluid flow over a solid object. Central to operation of the wind tunnel, a fan is used to move air over object(s) in a test area. Downstream of the test section there is often a means of recirculating the airflow back to the beginning of the tunnel. The recirculation zone can either be built into the wind tunnel or not. This choice subdivides wind tunnels into two primary varieties: open-return and closed-return, as seen in Figure 2. In open-return designs, the fan and test zone are placed in an open area, like a warehouse. Closed-return wind tunnels use a channel to return the air, meaning the wind tunnel is sealed.

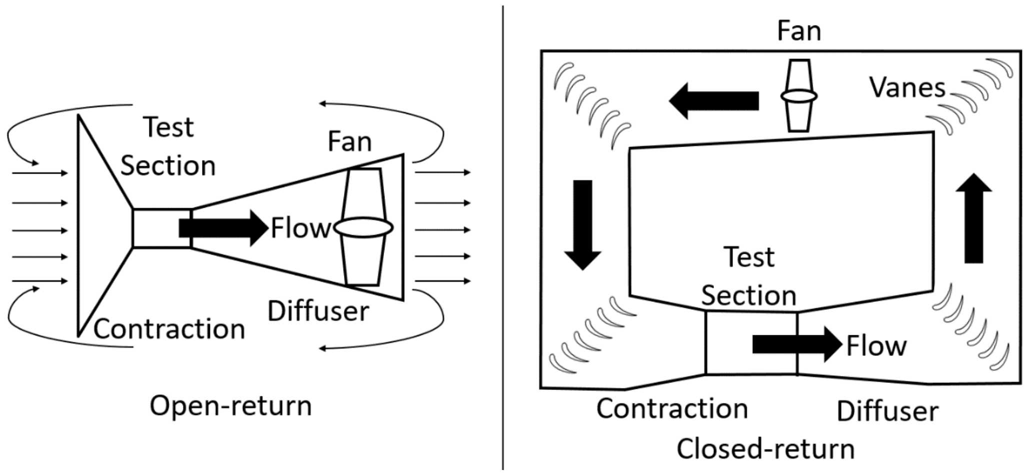

Figure 2. Illustration of an open-return versus a closed-return wind tunnel. An open-return wind tunnel does not have a direct channel that recirculates the flow, while a closed-return wind tunnel does.

Frank H. Wenham (1824-1908) is credited with designing and using the first wind tunnel in 1871 — 30 years before the Wright brothers. Wenham and his colleague, John Browning, made many valuable and fundamental findings. One such discovery is that at low angles of incidence (5 to 15 degrees), flat plates and airfoils can have a high lift-to-drag ratio, which allowed them to support higher loads than previously thought possible [1, 3]. The Wright brothers used these findings and many others to construct their own wind tunnel. A sketch of the wind tunnel used by the Wright brothers is shown in Figure 3 [1].

After the invention of the wind tunnel and validation of its benefits, aerodynamicists were able to conduct a much wider range of experiments using a variety of wind tunnels. Wind tunnel sizes range from large, like the V/STOL wind tunnel located at Langley (4.4 m x 6.6 m), to small, like the wind tunnel used by Thomas Stanton at the National Physical Laboratory in England (diameter of 0.61 m) [1]. Similarly, the types of studies completed in wind tunnels is extensive. For example, L. P. Chamorro and F. Porté-Agel conducted wind tunnel experiments to better understand flow patterns inside and above a model wind farm [4]. C. Chang and R. N. Meroney, on the other hand, studied pollutant flow in urban and open-country environments using wind tunnels and computational methods [5]. A. B. Bailey and J. Hiatt used measurements gathered from wind tunnels to comprehensively describe aerodynamic drag on spheres [6]. As a final example, G. B. Cosentino describes how wind tunnel results are compared to computational results to aid in the design of X-planes [7]. These examples provide an idea of the broad range of uses for wind tunnels in experimental aerodynamics.

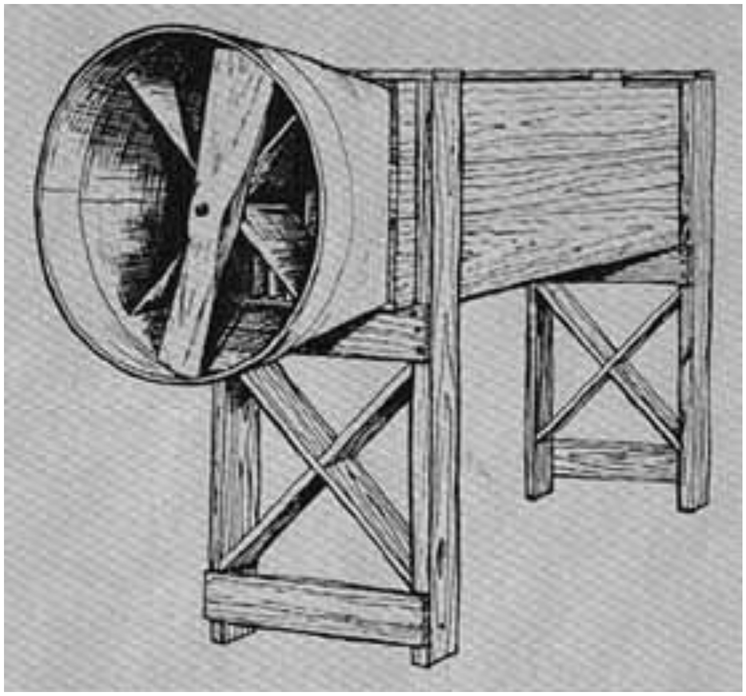

Figure 3. Drawing of the Wright brothers' wind tunnel design. The fan was powered by a small gas motor. Air was pushed through the tunnel by the fan. The Wright brothers found that the fan produced swirling motion inside the tunnel, which was challenging to avoid. Figure taken from Ref. [1].

1.2. Approaches to Fluid Mechanics

When approaching a fluid mechanics problem in the present day, there are three methods of finding a solution, whether exact or approximate: theoretical, computational, and experimental. Each method has its own benefits and flaws, which will be discussed in its respective subsection. By the end of this section, it should be clear that each method is valuable for certain applications, but no one method can stand on its own. This section references Tannehill et al. [8] in its discussion of the approaches to fluid mechanics.

1.2.1. Theoretical

The theoretical (or "analytical") approach, for a given problem, attempts to find a solution to the governing equations. These equations are obtained by applying the principles of conservation of mass, momentum, and energy to the motion of fluids. Boundary conditions specific to the problem are applied, and solutions are sought to the resulting partial differential equations.

The theoretical approach has multiple benefits compared to other methodologies. The biggest benefit is that a closed-form solution can sometimes be obtained by this method, meaning the results (e.g., velocity) are obtained as functions of parameters important to the problem (e.g., sizes of geometric features, viscosity, position, and time). This assists in engineering design, initializing a computational simulation, designing an experimental apparatus, etc. Further, the analytical solution can be used to validate results obtained using the other methods. For example, theoretical results for a given problem can be compared to those of a computer simulation for the same scenario. This comparison can help to check that the computer simulation has been performed correctly. The theoretical approach also helps fluid dynamicists build physical intuition. Understanding a basic problem that has an exact solution can help when approaching more complex problems that do not have exact solutions.

While the theoretical approach is a good starting point for understanding a given problem better, it does come with its disadvantages. A major drawback of the theoretical method is that the governing equations are a system of coupled non-linear partial differential equations that generally do not have an exact solution for a given scenario. For this reason, simplifying assumptions often must be made. Examples of assumptions include fully-developed flow, incompressible flow, time-independent flow, assuming flow is through an infinitely long pipe or an infinite channel, etc. [8]. If a solution is reached, it will likely only partially reflect real-world solutions to similar problems. For example, the solution to flow through an infinite pipe is accurate for long pipes but is less accurate for short ones.

1.2.2. Computational

Computational fluid dynamics (CFD) is a technique used to approximate the solution to the governing equations for a given fluid dynamics problem. To perform a CFD analysis for a certain problem, the fluid volume is first filled with a mesh. See Figure 4 for an example. Each cell in the mesh contains information (density, velocity, and pressure, etc.) about the fluid it encloses. Within each cell, the solution is assumed to be uniform. Throughout the mesh, the results are iteratively adjusted forward in time to determine the approximate solution to the problem. CFD requires significant computational power because it relies on numerical methods to find a solution.

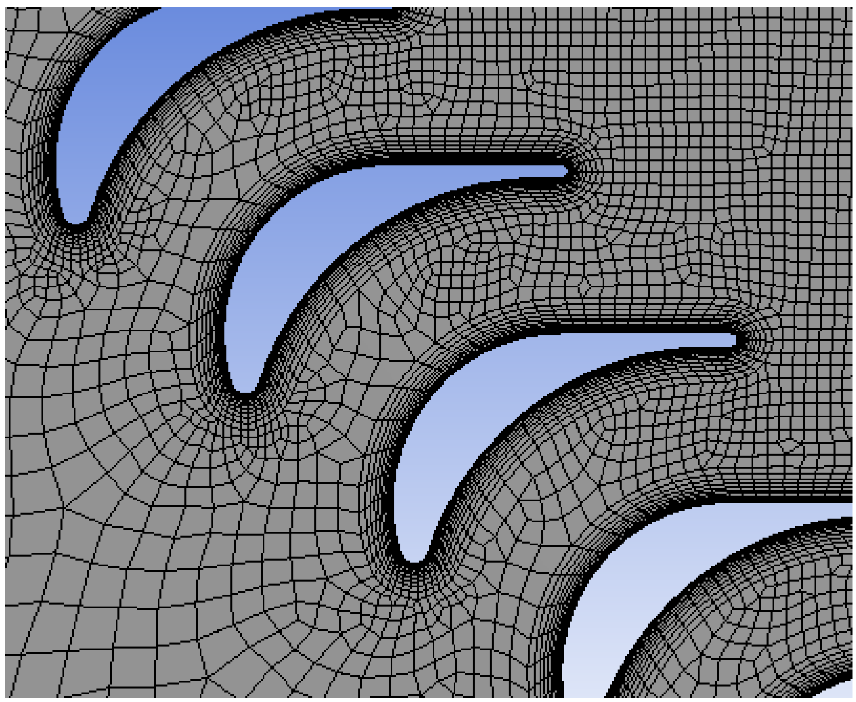

Figure 4. Example of what a mesh may look like for a CFD simulation. This image is from a simulation of air flowing through an array of vanes. Because the solution is assumed to be uniform in each cell, the mesh is made finer in regions where a larger solution gradient is expected, and coarser otherwise. Figure taken from simulation files produced by Eager [10].

The CFD method has many advantages that other methodologies lack. The biggest advantage is that approximate solutions can be obtained for any problem, including those for which there is no analytical solution. Furthermore, fewer physical assumptions are required compared to the theoretical approach. Another advantage is that when viewing the solution obtained by CFD software, information about variables such as air velocity or pressure at any location can easily be obtained. This is one of the reasons why CFD is generally cheaper than the experimental approach. In terms of computational resources, one only needs a decent desktop computer for many (but not all) applications. This saves a lot of time compared to setting up an experiment and taking measurements, making CFD cheaper in that instance.

CFD has its benefits, but it also comes with certain downsides. The largest problem with using CFD is accuracy. When testing a model, it is difficult to know how accurate the results are compared to the actual solution. Specifically, the accuracy of CFD simulations depends on the numerical techniques utilized, the quality of the mesh, accuracy of the modeling that is used (e.g., turbulence model), and the metric by which the simulation results are shown to converge. Each is elaborated upon below.

1. Numerical techniques are used to approximate the solution to partial differential equations like the governing equations of fluid dynamics [8]. There are numerous numerical techniques available, all with their own advantages and disadvantages. Some are more efficient than others, some are easier to implement, some are more accurate, etc. With the choice, however, there is typically a trade off between numerical accuracy and computational expense.
2. Mesh quality is affected by multiple features, but if a mesh is created with poor quality, the simulation will yield poor results. Generally, the mesh should be denser in regions where the solution is expected to have a larger gradient. That said, a mesh that is fine in the entire solution space is inefficient, so it must be created with this consideration in mind. Furthermore, the CFD practitioner should pay attention to mesh metrics that depend on the shape of the cells (e.g., cell skewness, aspect ratio). These also affect the accuracy of simulations.
3. Physical models are often used to simplify the computation, such as turbulence models, for example. However, it is often not clear how one should choose the best model for a specific application. Simulations are usually required using a variety of

turbulence models to see which produces the most accurate results when compared to experimental data.

4. Convergence metric is the metric by which the simulation is shown to converge and should be chosen carefully, as well. Commonly, changes in the solution as a function of iterations are monitored. For example, in predicting the lift on an airfoil, convergence may have been reached when the lift on the airfoil changes very little with each iteration. If not carefully analyzed, however, the lift may not be fully converged to the best solution.

Another problem with CFD — possibly the biggest — is computational expense. It is common for simulations to require the use of supercomputers, which are not cheap to purchase, set up, power, or maintain. This means the cost for running a CFD analysis can quickly increase if it must be run on a supercomputer. If computational power was not a problem, one could use more accurate numerical methods, use as fine a mesh as is required, use no turbulence model (or any other physical assumptions), etc. One could get arbitrarily better results with CFD if computational expense was not a problem.

1.2.3. Experimental

In the experimental method, a researcher directly measures relevant physical fluid properties. The typical process for conducting a fluid mechanics experiment involves designing and building a model to be tested in a wind tunnel. The model may include some means of measuring the desired information — such as air velocity, pressure, force, etc. If the model does not include such means, however, the wind tunnel must.

Like the previous methods, the experimental method has many advantages. If done correctly, the results are the most representative of those in the real world. This is by far the best advantage to the experimental approach. Like CFD, the experimental approach is applicable to many more problems than the theoretical method. However, it generally requires the least (potentially questionable) assumptions. Conducting an experiment, however, is not without its difficulties.

Often, some simplifying assumptions may need to be made about the situation being studied, as exact scenarios can be challenging to replicate in an experiment. A certain degree of extrapolation is often required, which introduces the possibility for results to be attributed to situations for which they are inaccurate. Another consideration for conducting a fluid mechanics experiment is that they can be costly. Wind tunnels can be expensive to build or get access to. Even if an experimenter has a wind tunnel available, designing an experiment takes a much longer time than the other approaches. The design of the model must be carefully planned and machined. For example, designing and building a scale aircraft that has holes running through it for pressure taps is not trivial. It also takes a long time to plan out how measurements will be made.

Finally, it should be noted that not one of the above methods is enough to fully understand and explore a given problem. Only a combination of theoretical solutions (if possible), CFD, and experiments can produce confidence that an accurate result has been obtained.

1.3. Objective

The goal of this project is to design and construct a small-scale, low-speed, closed-return wind tunnel to provide opportunities for new research and further education at Houghton College. This will significantly add to existing CFD capabilities at Houghton, allowing student researchers to approach fluid flow problems using different techniques. Examples of experiments that may be performed include tests on aircraft models and plasma actuators for active flow control. Future work will be discussed further in Chapter 5.

This thesis covers the general design of the wind tunnel and the steps taken to construct it. Empirical correlations were used by a previous researcher — Jonathan Jaramillo — to generate a preliminary design based on various constraints [9]. Examples of such constraints include the size of the room, the speed within the test section, and the desired flow quality. The preliminary design was further refined by Daniel Eager [10] and Jeremy Martin [11]. Eager conducted research on optimal spacing for the wind tunnel's corner vanes. Corner vanes are built into the corners of the wind tunnel to smooth flow through them. Martin worked on determining the best nozzle out of three candidates to use for the wind tunnel. Building on this previous work, specific attention is given in this thesis to the design and construction of the diffusers and two of the corners. Additional details for the other components of the wind tunnel will be presented and future work discussed.

The remainder of this thesis is outlined as follows. Chapter 2 will cover the theory of fluid mechanics, including the governing equations for fluid motion and the empirical correlations used to design the Houghton College wind tunnel. Chapter 3 discusses the initial design and refinement of the wind tunnel, which was completed by previous researchers. Chapter 4 focuses on the progress that has been made recently in the process of building the wind tunnel. Finally, Chapter 5 will present conclusions and future work for this project.

Chapter 2

THEORY

2.1. *The Governing Equations*

The equations that govern motion for a Newtonian fluid (e.g. air, water) are the continuity equation, Navier-Stokes equations, energy equation, equation of state, and equation for the internal energy of the fluid. Further information about the governing equations and their derivations can be found in Ref. [12].

First, what is known as the continuity equation is written as

$$\frac{\partial \rho}{\partial t} + \frac{\partial}{\partial x_k}(\rho u_k) = 0. \tag{1}$$

Note that Einstein's summation convention is being utilized in this and the following equations. In Equation (1), ρ is the mass density of the fluid, x_k represents the k^{th} spatial coordinate, u_k represents the k^{th} fluid velocity component, and t is time. Equation (1) is derived from the principle of conservation of mass applied to a moving fluid [8]. Second, the Navier-Stokes equations can be written as one formula that represents three equations — one for each value of the subscript *j*. They are written as

$$\frac{\partial(\rho u_j)}{\partial t} + \frac{\partial(\rho u_j u_k)}{\partial x_k} = \frac{\partial}{\partial x_i}\left\{-p\delta_{ij} + \mu\left(\frac{\partial u_i}{\partial x_j} + \frac{\partial u_j}{\partial x_i} - \delta_{ij}\frac{2}{3}\frac{\partial u_k}{\partial x_k}\right)\right\}. \tag{2}$$

The operator δ_{ij} is the Kronecker delta, μ is the fluid viscosity, and p is the fluid static pressure. Equation (2) represents Newton's Second Law applied to fluids [14]. If gravity or other body forces have an effect, there is an additional term added to account for the introduced forces. Because the fluid in question is air, the body force term (e.g. gravity) is generally small compared to the other forces. The static pressure takes the form $p = \rho RT$, the general representation of the thermal equation of state (i.e. the ideal gas law). In the thermal equation of state, the quantity T is temperature and R is the specific gas constant — the universal gas constant divided by the molar mass of the fluid. Because the ideal gas law is being used, it is assumed that the fluid behaves as an ideal gas with constant specific heats. Finally, the energy equation for a Newtonian fluid is

$$\begin{aligned}\frac{\partial}{\partial t}\left(\rho e+\frac{1}{2}\rho u_j u_j\right)+\frac{\partial}{\partial x_k}\left[\left(\rho e+\frac{1}{2}\rho u_j u_j\right)u_k\right]\\ =\frac{\partial}{\partial x_i}\left\{u_j\left(-p\delta_{ij}+\mu\left[\frac{\partial u_i}{\partial x_j}+\frac{\partial u_j}{\partial x_i}-\delta_{ij}\frac{2}{3}\frac{\partial u_k}{\partial x_k}\right]+\delta_{ij}k\frac{\partial T}{\partial x_j}\right)\right\}.\end{aligned} \tag{3}$$

The variables mentioned above are the same for this equation, with the addition of the thermal conductivity k and the specific internal energy of the gas e, written as

$$e = C_v T, \tag{4}$$

where C_v is the specific heat at constant volume.

It is beneficial to write the governing equations in a non-dimensional form. To do this, the variables ρ, p, u, x, T, and t are normalized as follows

$$\rho' = \frac{\rho}{\rho_\infty}, \quad u' = \frac{u}{U_\infty}, \quad p' = \frac{p}{\rho_\infty U_\infty^2}, \quad x' = \frac{x}{L}, \quad T' = \frac{T}{T_\infty}, \text{and } t' = \frac{U_\infty}{L}t. \tag{5}$$

In these expressions, a prime indicates a non-dimensional value, a subscript ∞ indicates a reference value, and L is a reference length. After substituting these non-dimensional variables into Equations (1), (2), and (3), the continuity equation becomes

$$\frac{\partial \rho'}{\partial t'}+\frac{\partial}{\partial x'_k}(\rho' u'_k) = 0, \tag{6}$$

the Navier-Stokes equations become

$$\frac{\partial(\rho' u'_j)}{\partial t'}+\frac{\partial(\rho' u'_j u'_k)}{\partial x'_k} = \frac{\partial}{\partial x'_i}\left\{-p'\delta_{ij}+\frac{1}{\mathrm{Re}}\left(\frac{\partial u'_i}{\partial x'_j}+\frac{\partial u'_j}{\partial x'_i}-\delta_{ij}\frac{2}{3}\frac{\partial u'_k}{\partial x'_k}\right)\right\}, \tag{7}$$

and the energy equation is

$$\frac{\partial}{\partial t'}\left(\frac{p'}{\gamma-1}+\frac{1}{2}\rho' u_j' u_j'\right)+\frac{\partial}{\partial x_k'}\left[\left(\frac{p'}{\gamma-1}+\frac{1}{2}\rho' u_j' u_j'\right)u_k'\right]$$
$$=\frac{\partial}{\partial x_i'}\left\{u_j'\left(-p'\delta_{ij}+\frac{1}{\mathrm{Re}}\left[\frac{\partial u_i'}{\partial x_j'}+\frac{\partial u_j'}{\partial x_i'}-\delta_{ij}\frac{2}{3}\frac{\partial u_k'}{\partial x_k'}\right]\right.\right. \tag{8}$$
$$\left.\left.+\frac{1}{(\gamma-1)\mathrm{Pr}\mathrm{M}^2\mathrm{Re}}\delta_{ij}\frac{\partial T'}{\partial x_j'}\right)\right\},$$

where γ is the specific heat at constant pressure divided by the specific heat at constant volume [13]. Lastly, non-dimensionalizing the ideal gas law,

$$p'=\frac{\rho' T'}{\gamma \mathrm{M}^2}. \tag{9}$$

Upon writing these equations in dimensionless form, three dimensionless quantities appear: Re, M, and Pr. They are known as the Reynolds number, the Mach number, and the Prandtl number, respectively. These are referred to as similarity parameters. Two non-dimensional solutions for flow over geometrically alike bodies will be identical if the similarity parameters for both situations are the same [13]. They are defined as

$$\mathrm{Re}=\frac{\rho_\infty U_\infty L}{\mu_\infty}, \tag{10}$$

$$\mathrm{M}=\frac{U_\infty}{a_\infty}=\frac{U_\infty}{\sqrt{\gamma R T_\infty}}, \tag{11}$$

and

$$\mathrm{Pr}=\frac{C_p\mu}{k}. \tag{12}$$

In the above equations, C_p and a_∞ are respectively the specific heat of air at constant pressure and the speed of sound in the fluid. The Reynolds number, Re, expanded upon below, is the similarity parameter of interest in low-speed wind tunnel applications. It is a coefficient that is inversely proportional to the strength of viscous forces. On the other hand, the Mach and Prandtl numbers affect the governing equations in multiple places (e.g., the ideal gas law and the thermal conduction term in the energy equation). The Mach number is the ratio of the reference speed and the reference speed of sound, whereas the Prandtl number is a temperature dependent property of the fluid.

For low-speed wind tunnels, it can be shown that fluid density is approximately constant when the Mach number is less than 0.3. Because of this, there are seven equations with only six unknowns (fluid velocity in three directions, fluid pressure, temperature, and internal energy). Because density is now known, the energy equation may be omitted. Therefore, the only equations that need to be considered are Equations (6) and (7). Thus, for problems with a Mach number less than about 0.3, the Reynolds number is the most important similarity parameter, as it is the only one represented in the non-dimensional governing equations [14]. The maximum Mach number in the Houghton College wind tunnel will be approximately 0.13, with a reference speed of sound of 343 m/s (at 20 °C). This justifies the incompressible flow assumption.

2.2. Empirical Correlations for Wind Tunnels

There are certain relationships, determined experimentally, that aided in the preliminary design of the wind tunnel. General guidelines are considered here, as well as necessary info on quasi-one-dimensional flow. Finally, empirical correlations for many types of wind tunnel components will be covered. Ref. [14] provides helpful information on these topics. The following discussion will focus on information that is most relevant to closed-return, small-scale wind tunnels.

2.2.1. General Guidelines

Referring to Figure 5, the following paragraph will discuss the general design guidelines for closed-return wind tunnels. These guidelines are discussed in further detail in Barlow et al. [14] and Bradshaw [15]. First, the test section (a) can be partially or fully open, closed, or convertible. The ratio between the test section length and its hydraulic diameter is usually more than 2. For a circular cross-section the hydraulic diameter is simply the diameter, but for a rectangular cross section it is defined by Blevins [16] as

$$D_h = \frac{2\ell w}{\ell + w}, \tag{13}$$

where ℓ and w are side lengths. There is typically a diffuser (b) after the test section that has a length of at least three or four test section lengths. The area ratio should be between 2-3 and the cone angle between 2-3.5°. For both measurements, smaller is better. Next, there is a corner (c) with turning vanes incorporated into it. After the corner, there is a section (d) that may have constant area or be a diffuser. Between component (d) and the next corner there should be a screen (e) to catch any loose parts that could pass through the fan. For example, this could stop pieces of a model if it were to break during testing. Next, there is generally another corner (f) with turning vanes, then a transition (g) from a square cross-section to a circular one, to take fluid into the fan smoothly. A straightener section (h) is commonly incorporated after the fan to straighten the flow. Next, the second diffuser (i) (or third diffuser if section (d) is used as a diffuser) often includes a transition from a circular cross-section to a rectangular cross-section. This diffuser should have the same dimension constraints as the first diffuser (b). After the second diffuser, there is typically another corner (j) with turning vanes, a constant area section (k) or another diffuser, then a heat exchanger (l), and one last corner (m) again with turning vanes. After the fourth corner, a wide-angle diffuser (n) with separation control screens is used to slow air down before going through the settling area (o). The wide-angle diffuser commonly has a cone angle of about 45° and an area ratio between 2-4. Next, the flow is conditioned at (p) using flow straighteners and turbulence control screens. Finally, the nozzle (q) connects to the test section. The nozzle typically has an area ratio between 7-12, but lower and higher values have been used before.

2.2.2. Quasi-One-Dimensional Flow

One principle which is helpful in the preliminary design of wind tunnels is that of quasi-one-dimensional flow. Anderson [13] discusses this idea in greater depth — the results of his discussion are presented here. When considering flow through a duct, if one assumes that the flow variables are functions of one dimension only (i.e., functions of x, the primary direction of motion through the duct), the quasi-one-dimensional continuity equation is [13]

$$\rho A U = \text{constant}, \tag{14}$$

where ρ is the density of the fluid, A is the cross-sectional area of the duct, and U is the cross-sectional fluid velocity. According to the quasi-one-dimensional assumption, $\rho = \rho(x)$, $A = A(x)$, and $U = U(x)$. Equation (14) is an expression stating that the mass flow through the duct remains constant. For incompressible flow, which is approximately true if the Mach number is less than 0.3, Equation (14) becomes

$$AU = \text{constant}. \tag{15}$$

This is the quasi-one-dimensional continuity equation for incompressible flow [13]. It states that for a duct, the volume flow rate is constant. In other words, the average fluid velocity is inversely proportional to the cross-sectional area of the duct at that location.

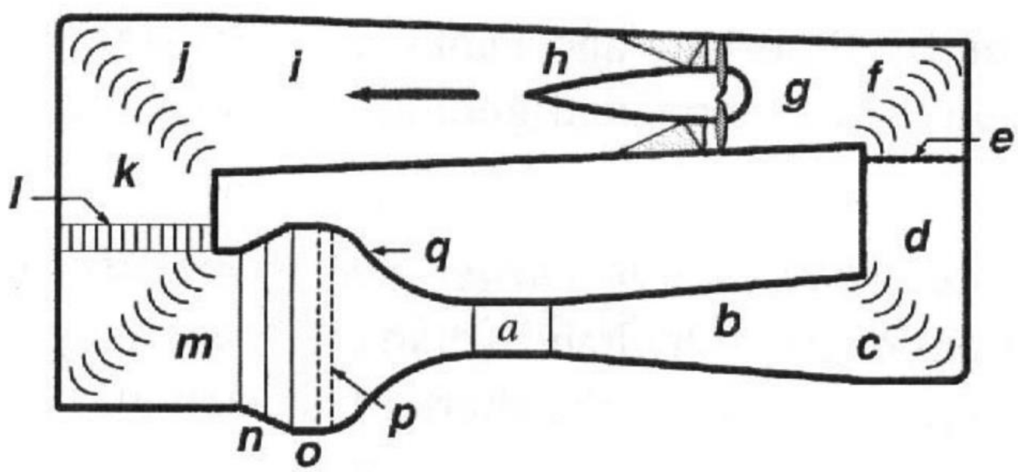

Figure 5. The general layout of a closed-return wind tunnel. Starting at *a*, the test section, fluid flows counter-clockwise around the tunnel. Figure taken from Barlow et al. [14].

2.2.3. Section Pressure Loss Coefficients

The next section will discuss what are known as section loss coefficients for each wind tunnel component. As fluid moves through the wind tunnel, it experiences a stagnation pressure drop due to friction at solid surfaces and separation, if it occurs. The stagnation pressure increase at the fan must balance out the sum of the stagnation pressure losses around the tunnel. Refer to Figure 5 for a depiction of a typical closed-return wind tunnel. These losses can be thought of as inefficiencies, and the loss coefficient is defined as

$$K_i = \frac{\Delta p_{oi}}{q_i} \tag{16}$$

where subscript i denotes a specific wind tunnel component, Δp_{oi} is the stagnation pressure drop through the component, and q_i is the dynamic pressure of the fluid there [17]. Dynamic pressure is the kinetic energy per unit volume of a fluid. It is defined as

$$q = \frac{\rho U^2}{2}, \tag{17}$$

where U is the fluid velocity. Based on dimensional analysis, it is expected that Δp_{oi} for a component will be proportional to the fluid velocity in the component squared. Therefore, this allows models for the loss coefficient to be developed for different components. To balance out these section losses and reach the desired speed in the test section, the fan must input power into the flow. This is calculated by

$$P_{\text{required}} = \left(\sum_{i=1}^{N} K_i \frac{q_i}{q_t}\right) \frac{\rho_t^2 A_t U_t^3}{2 \rho_F \eta_F}, \tag{18}$$

from Eckert et al. [17]. Here, the summation is over all components of the wind tunnel. The value q_t is the dynamic pressure of the test section. The variable A_{t} is the cross-section area of the test-section, U_t is the flow velocity of the test section, and η_{F} is the aerodynamic efficiency of the fan/motor system. A conservative value of $\eta_{\mathrm{F}} = 0.8$ was used for this project based on the discussion in Ref. [15]. For incompressible flow, ρ_{t}, the density in the test section, is equal to ρ_{F}, the density in the fan.

In the early design of a wind tunnel, empirical correlations for the K_{i} coefficients in Equation (16) are often utilized. For general information about this approach, see the discussions presented by Barlow et al. [14] and Eckert et al. [17]. For information specific to the Houghton college wind tunnel, see the thesis written by Jonathan Jaramillo [9]. Important coefficients for the design of the Houghton College wind tunnel are given below.

For constant-area sections, the pressure loss coefficient is given by

$$K = \frac{\lambda L}{D_h}, \tag{19}$$

where K is the pressure loss coefficient, D_h is the hydraulic diameter (defined in Equation (13)), λ is the friction coefficient for a smooth pipe, and L is the centerline length [17]. The friction coefficient is defined

$$\frac{1}{\sqrt{\lambda}} = 2\log_{10}\left(Re\sqrt{\lambda}\right) - 0.8, \tag{20}$$

where Re is the Reynolds number for the section, calculated using the section's mean speed and hydraulic diameter at the upstream end of the section. This equation is iteratively solved to approximate λ [14]. The loss coefficient for constant-area corners is given by Barlow et al. [14] as

$$K_c = 0.10 + \frac{4.55}{(\log_{10} Re_c)^{2.58}}, \tag{21}$$

where the Reynolds number, Re_c, is based on the corner vane chord length and the mean flow speed through the corner. For diffusers, the loss coefficient is approximated as

$$K = \left[K_{ex} + \left(\frac{\lambda}{8\sin\theta}\frac{\mathrm{AR}+1}{\mathrm{AR}-1}\right)\right]\left(\frac{\mathrm{AR}-1}{\mathrm{AR}}\right)^2. \tag{22}$$

In the equation, K_{ex} is the expansion loss coefficient — representing losses due to expansion of the diffuser, θ is the angle of expansion of the diffuser, and AR is the area ratio. The second term in Equation (22) represents losses due to friction. Expansion loss coefficients for different types of diffusers are experimentally determined, and more detail about them can be found in Barlow et al. [14] and Eckert [17]. The angle of expansion is calculated using

$$\theta = \arctan\left(\frac{1}{2}\frac{\sqrt{\mathrm{AR}}-1}{L/D_1}\right). \tag{23}$$

In Equation (23), AR is the cross-section area ratio, D_1 is the hydraulic diameter at the upstream end, and L is the length of the diffuser [9]. Finally, Ref. [17] discusses expressions for screen loss coefficients based on porosity, which depends on wire diameter and weave density, d_m and w_m, respectively. Porosity is then written

$$\beta_s = \left(1-\frac{d_w}{w_m}\right)^2. \tag{24}$$

Using the porosity, the loss coefficient for a screen is

$$K_m = K_{mesh}K_{Rn}\sigma_s + \frac{\sigma_s^2}{\beta_s^2}. \tag{25}$$

These equations, and others, were used in an Octave script to calculate dimensions of various components given certain constraints and to estimate the specifications for the fan to be able to reach speeds of 44.7 m/s (100 mph) in the test section [9]. The initial design of the Houghton College wind tunnel and subsequent refinements are discussed in the next chapter

Chapter 3

WIND TUNNEL DESIGN

3.1. Initial Design

The initial design for the wind tunnel was decided on based on a few factors such as the size of the enclosing room, cost, energy efficiency, noise, etc. The size of the room constrained the tunnel to fit within a 4.57 m (15 ft) by approximately 2.3 m area, for example. Several initial design decisions were made based on these factors, which will be covered in the following section. For further information on the design of this wind tunnel, the work done by a previous student, Jonathan Jaramillo, can be found in Ref. [9]. Much of the content in this section is covered in Jaramillo's thesis in greater detail.

The first design choice was whether the tunnel should follow a closed circuit or an open circuit design. Open circuit wind tunnels cost less to build, take less time to build, and are good for testing systems with exhaust, but they are noisy and less energy efficient [9]. Because the wind tunnel will be inside an academic building, noise is an important factor. Closed circuit wind tunnels are more energy efficient, less noisy, and their flow quality can be controlled using screens and other flow-straightening components. There are problems with closed-circuit wind tunnels, however. For example, there is no easy way to remove smoke flow in the tunnel and they have a higher initial cost. A closed-circuit design for the Houghton College wind tunnel, as outlined in Chapter 2, was chosen for a few reasons. First, for the same test section size and maximum speed, an open-circuit design would be less efficient and have less flow uniformity due to the ends of the tunnel being near a wall [14]. Second, proximity to other classrooms and offices meant that a quieter wind tunnel design was preferable.

Contrary to the general closed-circuit wind tunnel layout given in Figure 5, the Houghton College wind tunnel will not include a heat exchanger or a wide-angle diffuser. A heat exchanger will not be needed because the air flowing through the wind tunnel is not expected to reach temperatures that will require such a device. The wide-angle diffuser, on the other hand, was not included in the design because the space in which the wind tunnel will fit does not have room for a wide-angle diffuser [9].

The preliminary design of the wind tunnel (see Figure 6) was determined by applying various physical constraints, empirical correlations, and known dimensions to an Octave script. (Octave is an open-source version of the numerical computing language MATLAB.) The script calculated section power-losses (detailed in 2.2.3, page 20), component lengths, and other information based on the parameters mentioned previously [9]. Initial design of the wind tunnel only consisted of component volumes and general dimensions — further development would come later.

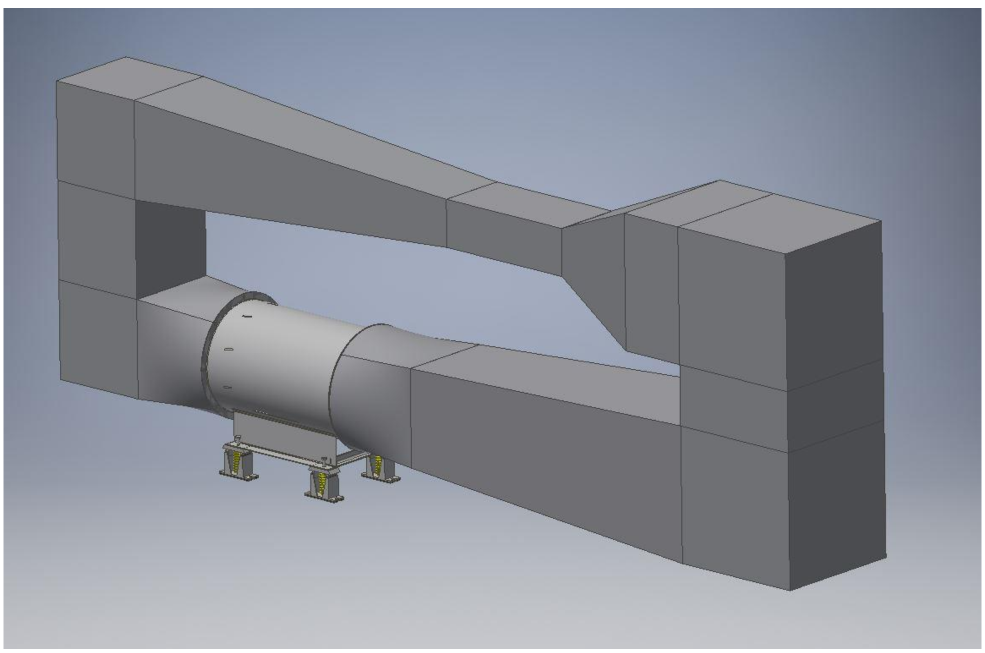

Figure 6. Initial design of the Houghton College wind tunnel. Airflow is in the counter-clockwise direction, and the test section is the narrowest section on top of the image. The preliminary design of the wind tunnel still required many refinements to be made, with the exception of the fan details. The motor and fan were purchased based on calculations completed by Jaramillo [9].

Once the general dimensions of the wind tunnel were determined, the material that would make up the wind tunnel had to be selected. Medium density overlay (MDO) plywood with a thickness of 19.1 mm (3/4 in.) was chosen for many of the sides of the tunnel. MDO plywood has a smooth side and is structurally stable. This is perfect for the wind tunnel because the pressure inside will often be higher than atmospheric, and the smooth sides of the plywood will reduce friction losses. For the side of the tunnel facing the operator, 13 mm (1/2 in.) thick plexiglass is used. Built this way, an observer can see the inside of all wind tunnel components, and each component should be structurally sound. Being able to see inside the wind tunnel will be helpful because the wind tunnel operator could immediately tell if there is a problem (e.g., a component breaking), and it allows visualization studies of the entire wind tunnel (e.g., smoke flow visualization). A Unistrut frame which would support the wind tunnel was also constructed. For further information about the Unistrut frame, see Ref. [9].

3.2. Initial Design Refinements

Upon preliminary design of the wind tunnel, the design was further refined through additional studies. Eager [10] performed CFD analyses to determine the optimal number of turning vanes to put in each corner. Turning vanes are built into the corners of a wind tunnel to reduce losses by keeping airflow smooth as it travels around a corner. Martin [11] conducted research on the shape of the nozzle by using CFD simulations. Each of these studies is elaborated upon in sections 3.2.1 and 3.2.2.

3.2.1. Corner Design

The difficulty in designing the corner vanes of a wind tunnel comes from choosing a shape for the vanes and choosing an appropriate chord-to-gap ratio [14]. Vanes can vary from bent metal plates to highly cambered airfoils. Type A — a double-walled vane — from Figure 7 was chosen for the Houghton College wind tunnel for several reasons. First, Krober [18] makes a note that for a Reynolds number of about 110,000 and a speed of about 28 m/s, a double-walled vane is the most efficient. The Reynolds number here is calculated based on a vane chord length of 59.3 mm. (Note that Krober originally reports a Reynolds number of 40,000, but it is unclear how this was calculated.) The chord-based Reynolds numbers for the Houghton College wind tunnel are 93,000 for the smaller corners and 49,000 for the larger corners. Second, vanes like these can be purchased easily from an HVAC supply seller. The vanes used here were manufactured by Aero Dyne [9]. This is much easier than bending sheet metal to create vane B or C.

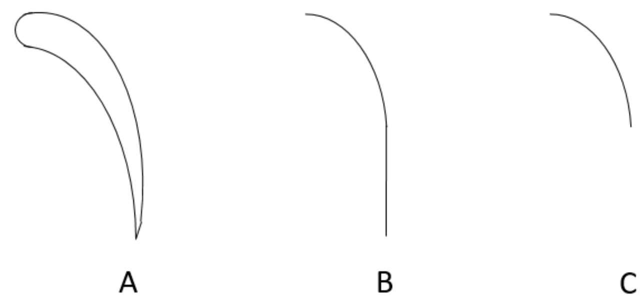

Figure 7. Cross sections of different types of corner vanes. Vane A has a blunt leading edge, referred to generally as a double-walled vane. These are generally more effective for flow-turning purposes. Vanes B and C are single-walled, formed from a single piece of metal. Figure adapted from Barlow et al. [14].

After the type of vane was chosen, the optimal number of vanes in each corner needed to be determined. There are many resources available for determining optimal spacing when using single-walled vanes [19]. This is because there are only a few configurations for the cross-section of a single-walled vane. However, there are many more possible airfoil shapes for double-walled vanes, and each possibility has its own optimal spacing. Eager [10] performed CFD analyses of the corners of this wind tunnel to determine the optimal vane spacing. Eager's simulations utilized ANSYS Fluent using the realizable k - ϵ turbulence model and Menter-Lechner near-wall treatment. An example of two of the meshes used in Eager's simulations is shown in Figure 8 [10].

Eager performed a variety of simulations with different numbers of turning vanes in each. Grid-refinement studies were also completed to ensure that the results were independent of the chosen mesh. The corner design with the lowest stagnation pressure loss was chosen. From this method, the first and second corners after the test section (corners 1 and 2) were designed to have 13 vanes [10]. With this number, the simulated pressure loss was 23.83 Pa. This is under the predicted 25 Pa calculated from the correlation used to estimate the loss for corners (Equation (21)), but still good given the approximate nature of the utilized empirical correlations. A value of 19 vanes was found to be the optimal number for the two corners immediately before the test section (corners 3 and 4). With this number of vanes, the simulated pressure drop is 6.91 Pa [10], compared to the calculated value of 7.32 Pa. The method used to physically install the vanes will be covered in Chapter 4.

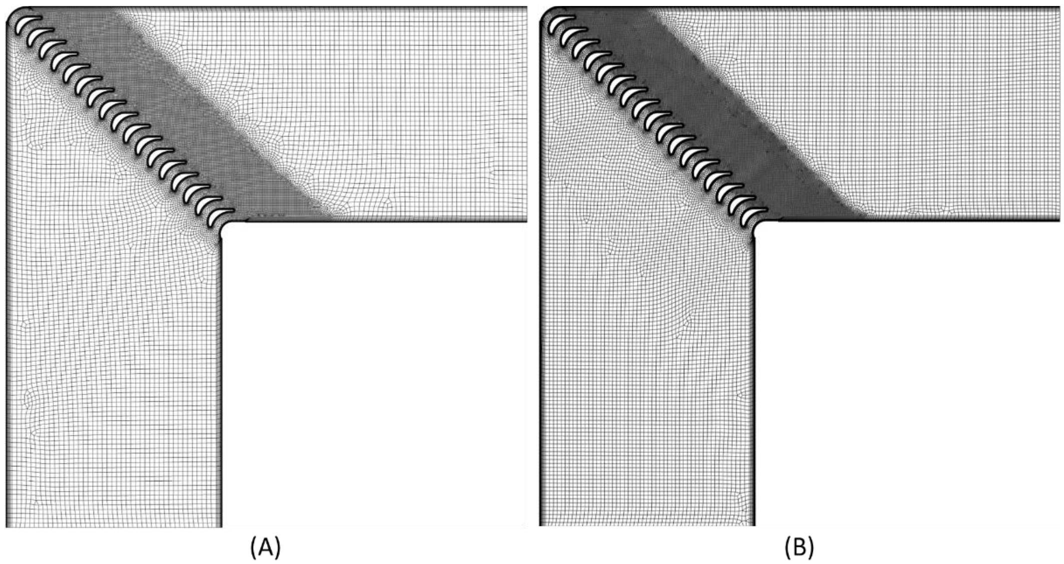

Figure 8. Examples of two meshed corners with different mesh refinements. These are the larger corners (3 & 4) of this wind tunnel. Air flows from the bottom of the image up to the blunt edge of the turning vanes, then exits to the right. Note that the mesh for both refinements is considerably finer after the airflow has passed the vanes and near the surfaces of walls to calculate the solution in those areas with greater accuracy. Figure taken from Ref. [10].

3.2.2. Nozzle Design

The nozzle of a wind tunnel works as a funnel for fluid moving from the settling chamber to the test section. It decreases in cross-sectional area in the direction of fluid flow, meaning flow through the test section has a much higher velocity than that through the settling chamber. Nozzles can increase the average fluid speed by up to 20 times or more, though this factor is generally in the range of 6-10 [14]. Referring to the quasi-one-dimensional continuity equation (Equation (15)), the fluid velocity in the component is inversely proportional to the cross-sectional area of the component. A general design for a nozzle is given in Figure 9 below.

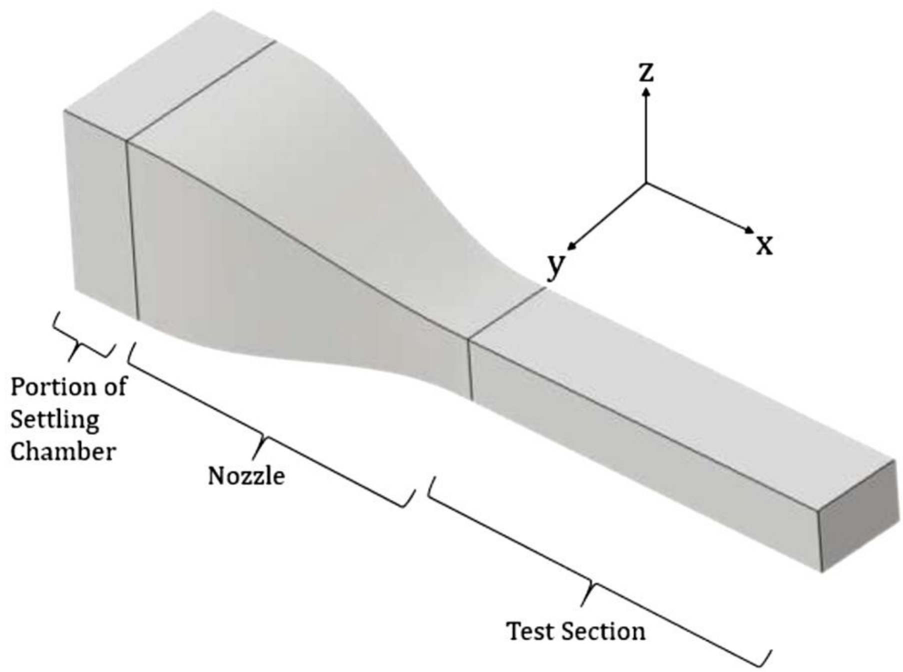

Figure 9. Diagram of a nozzle. The settling chamber and test section are also shown. Note that this depicts only a quarter of the entire volume. Because of symmetry, the section shown here can be mirrored about its lower XY plane and its XZ plane. Figure taken from Ref. [11].

To choose a nozzle design for the Houghton wind tunnel, CFD software (ANSYS Fluent) was used to run various simulations for different nozzle shapes. Three nozzles were considered. The first was proposed by Bell and Mehta [20], the second by Brassard [21], and the third by Morel [22]. A graph of the different nozzle profiles is given in Figure 10. For more information on the nozzle profiles and how they are defined, see Ref. [11].

All simulations computed by Martin used the realizable $k - \epsilon$ turbulence model with Menter-Lechner near-wall treatment and the coupled pressure-velocity scheme found in ANSYS Fluent 17.1 — the software used to perform the simulations. Flow was assumed steady and incompressible. Martin considered stagnation pressure drop through the nozzle and flow uniformity when evaluating each nozzle. Based on these measures, Martin determined that the Brassard nozzle is the best for this wind tunnel both in terms of stagnation pressure drop and flow uniformity [11]. However, the Brassard nozzle only performed marginally better than the others.

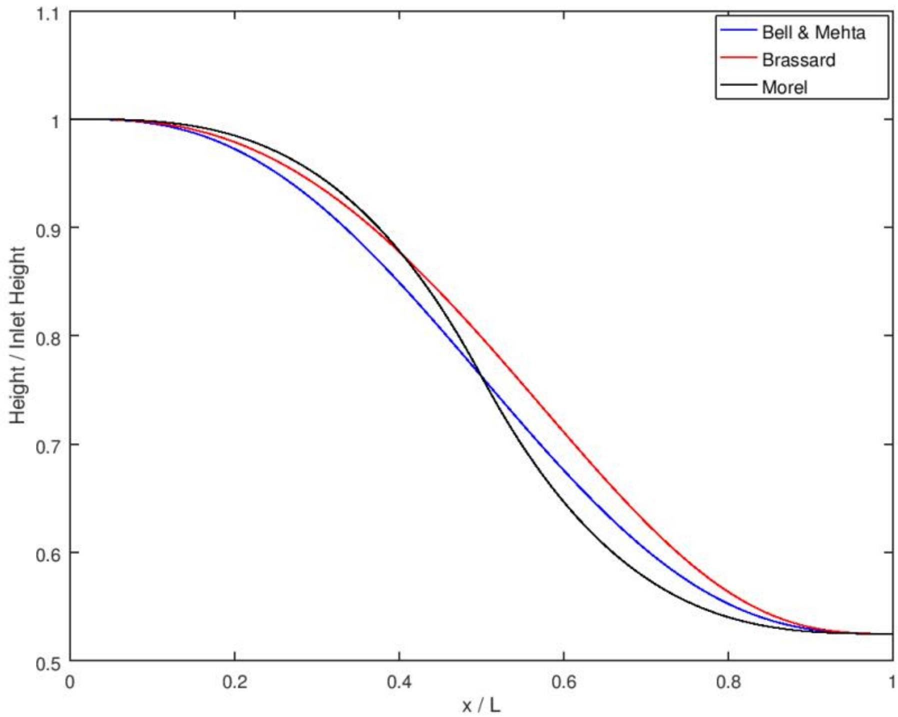

Figure 10. Graph of nozzle profiles. x is the distance from the start of the test section, and L is the length of the test section. Figure taken from Martin [11]. Data taken from Bell & Mehta [20], Brassard [21], and Morel [22].

Chapter 4

RESULTS

4.1. *Current Design Refinements*

The design of the wind tunnel has been refined considerably since the preliminary design work done by Jaramillo [9]. Design modifications and additional considerations will be discussed in this section. For the sake of clarity, components are numbered according to their distance downstream from the test section. This numbering system is illustrated in Figure 11 below. By this convention, diffuser 1 immediately follows the test section, while diffuser 2 is further downstream, after the fan. The corners work in the same way.

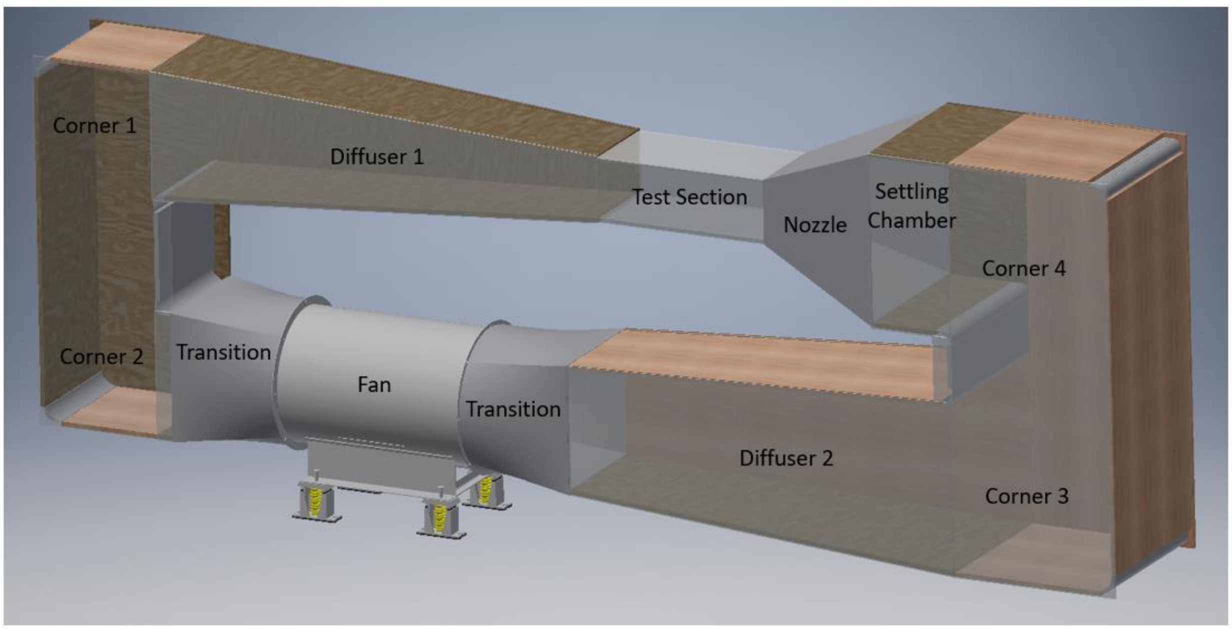

Figure 11. Diagram of the Houghton College wind tunnel's naming system.

The first modification was to shorten diffuser 2. As shown in Figure 12, the turning vane furthest inside corner 2 intersected with the transition attached to the fan. This happened because the dimensions of the corner vanes were not considered when the initial design of the wind tunnel was completed. Once they were added to the geometry, they required more space.

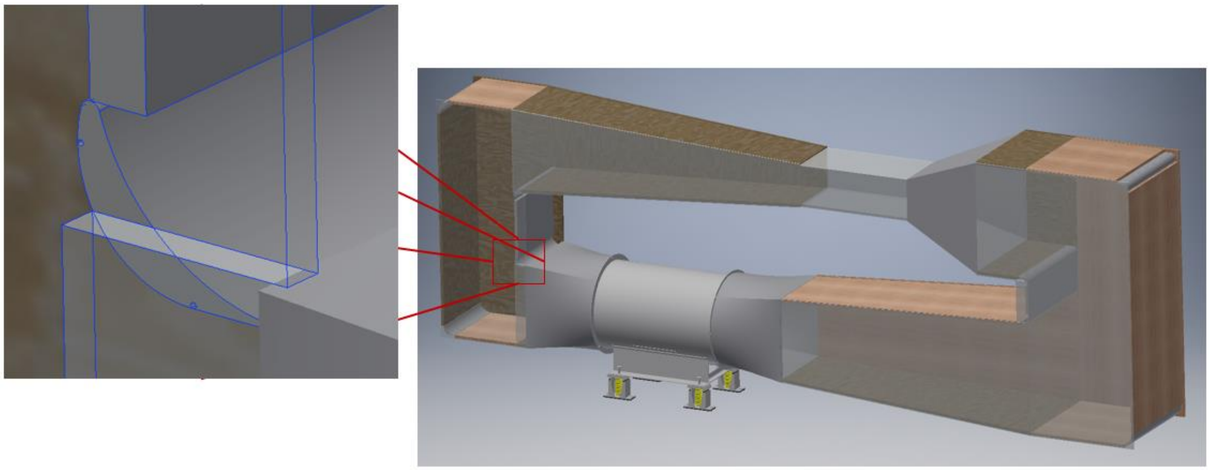

Figure 12. Image displaying the vane that intersected with a transition piece. The left image shows a zoomed-in view of the vane and transition not intersecting, and the image on the right shows the entire wind tunnel. Because of this vane, diffuser 2 (the bottom diffuser) had to be shortened.

A transition is a duct piece that is square on one end and circular on the other. These are necessary for this wind tunnel because the fan has a circular cross-section while the other parts of the wind tunnel have square cross-sections. The transition is metal and not easy to modify, and the turning vane also could not be cut to make room, so diffuser 2 had to be shortened by 7.2 cm to a length of 173.5 cm.

The decision to shorten the diffusers, if not made carefully, can result in flow separation and additional losses. Separation occurs when the flow detaches from the wall of the diffuser, leaving a region of recirculating flow near the wall. This phenomenon is illustrated in Figure 13. Flow separation is not desirable in a diffuser because it dramatically increases losses and promotes flow nonuniformity and unsteadiness [16].

To ensure that the decision to shorten a diffuser will not result in losses due to flow separation, the work done by Blevins [16] was consulted. In his book, there is a graph of area ratio (minus one) versus non-dimensional length for annular, conical, and two-dimensional diffusers (see Figure 14). The graph is gathered from experimental data [23, 24, 25]. Area ratio is defined in [16] as

$$\text{AR} = \frac{A_2}{A_1}, \tag{26}$$

where A_2 is the cross-sectional area of the downstream end of the diffuser, and A_1 is the area of the upstream end. Non-dimensional length is defined as

$$L' = \frac{N}{R_1}, \tag{27}$$

where N is the diffuser length and R_1 is half of the hydraulic diameter of the upstream end of the diffuser (see Equation (13)).

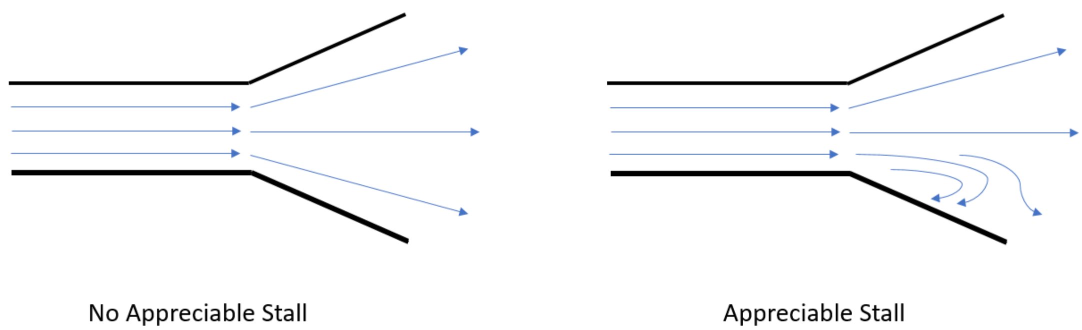

Figure 13. Image depicting the formation of flow separation in a diffuser. Airflow is indicated by arrows. Figure adapted from Blevins [16].

With these equations, the area ratio and non-dimensional length of diffuser 2 (before shortening) are calculated to be 1.91 and 7.30, respectively. A conical diffuser expands with a conical shape from its upstream end to its downstream end, much like diffuser 2, except it has a square cross-section. Assuming the line of first appreciable stall (or separation) for a conical diffuser in Figure 14 from Blevins [16] can be safely approached, diffuser 2 can be shortened down to a minimum length of 57 cm, from an original length of 180.7 cm. With this information, the decision for diffuser 2 to be shortened by 7.2 cm was validated.

The second modification to be made was to shorten diffuser 1 to allow for more screens in the settling chamber. A settling chamber holds screens in it which are used to make the flow more uniform before it reaches the nozzle. Often, a settling chamber also contains a honeycomb which further straightens the flow direction. Using more screens improves flow quality at the expense of making the settling chamber longer. The Houghton College wind tunnel design includes a settling chamber with three screens. The settling chamber was originally designed to be 34.0 cm (13.4 in.) long, but because a turning vane cuts into the chamber and a honeycomb has been added to the design, it needed to be lengthened. Barlow et al. [14] recommend a screen spacing based on wire diameter of about 500. The wire diameter for the screens that will be utilized here is 0.023 cm (0.009 in.). Therefore, each screen should have a space of about 11.4 cm (4.5 in.) that follows it. Along with this, the wind tunnel requires 5.1 cm (2 in.) for the honeycomb, and 7.1 cm (2.8 in.) for the turning vane. So, the settling chamber needs to be at least 46.5 cm (18.3 in.) long. This means that diffuser 1 must be shortened by 12.5 cm (4.9 in.) to a length of 180.0 cm. Using the equations above and Figure 14, diffuser 1 can be shortened to a minimum length of 93.3 cm from an original length of 192.4 cm and an area ratio of 2.85. Diffuser 1 has a non-dimensional length of 13.5 before shortening, and a non-dimensional length of 12.6 after shortening. Diffuser 1 only needs to be shortened by 12.5 cm (4.9 in.) the decision to shorten it is a safe one.

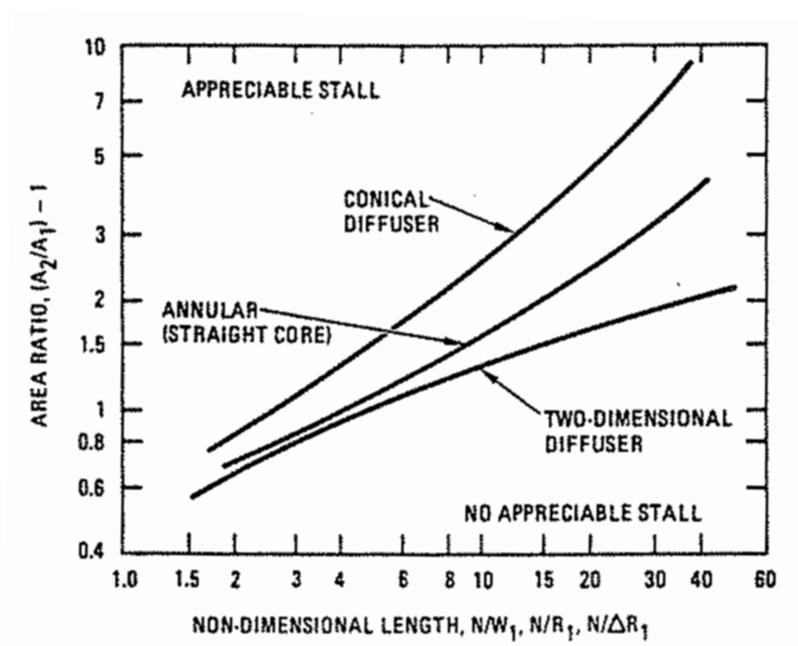

Figure 14. Relationship between area ratio and non-dimensional length for stall. This is gathered from three different experimental analyses for three types of diffusers [23] [24] [25]. Figure taken from Blevins [16].

4.2. Construction

4.2.1. Building Diffuser 2

To start constructing diffuser 2, each part was first cut out of a large piece of medium density overlay plywood (described in Chapter 3, Section 1). The shape of diffuser 2 is shown in Figure 15. The pieces of diffuser 2 are referred to as top, bottom, plexiglass, and back (i.e., the side opposite the plexiglass). The plexiglass and back pieces are slightly wider to allow for holes to be drilled through them and into the top and bottom pieces. The top piece is shorter than the other parts because of the innermost turning vane for corner 3. A list of the exact dimensions is given below in Table 1. For a list of all wind tunnel components and their dimensions, see Ref. [9].

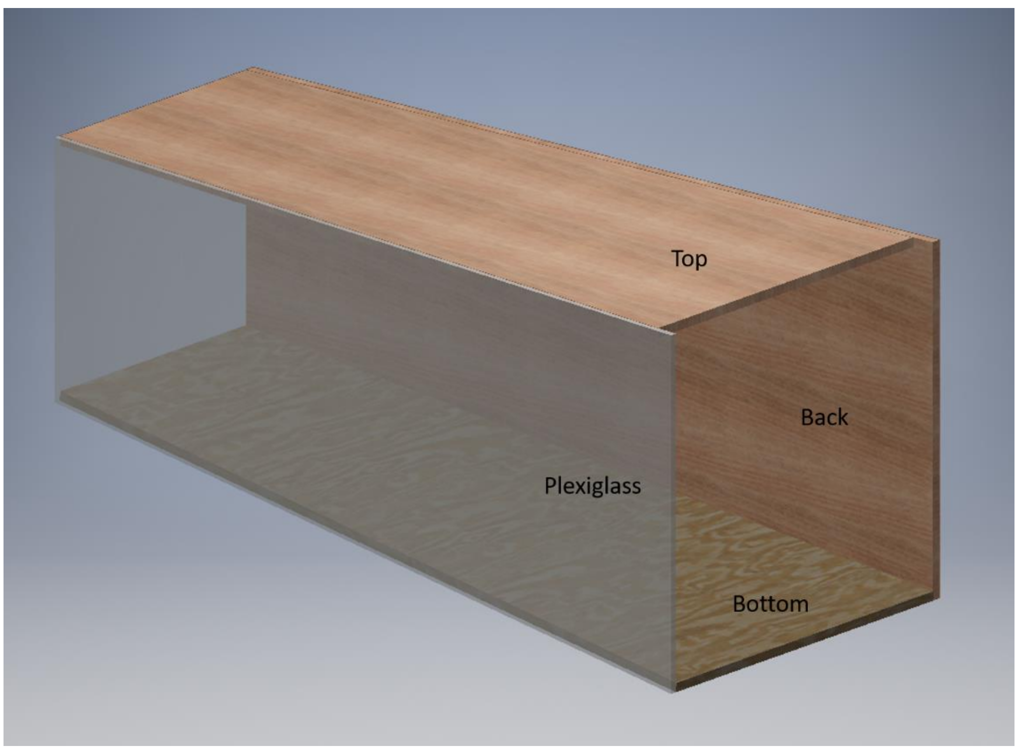

Figure 15. Image of diffuser 2. Note that the top part is slightly shorter, to make room for the turning vane at that point.

Table 1. A list of the dimensions of each part in diffuser 2. Length is measured perpendicular to the ends of each part. Each dimension is the final dimension.

Part Name	**Length (cm)**	**Upstream Width (cm)**	**Downstream Width (cm)**
Top	168.7	49.5	67.9
Bottom	173.7	49.5	68.4
Plexiglass	173.7	53.3	72.2
Back	173.7	53.3	72.2

Once each piece was cut, they were assembled using 8 x 2 in. Phillips Flat Twinfast Cabinet Screws at approximately 10.2 cm (4 in.) intervals. 100% Gorilla silicone sealant/caulk was used to smooth and seal the inner corners after the diffuser was finished. This should reduce air leakage in the corners of the diffuser. It is important to seal these cracks because if air is leaking out of the tunnel, the pressure — which will be equal to or higher than atmospheric throughout the tunnel — would decrease locally, meaning the energy of the flow field would decrease overall.

During the process of construction, a few problems had to be resolved. The circular saw used to cut the pieces of the diffuser required a new saw blade — a Concord 7-1/4-Inch 80 teeth metal saw blade. This was necessary to cut through the plexiglass side without chipping it. The new saw blade had 40 more teeth than the previously used blade, allowing it to cut through plexiglass with ease. Once construction of diffuser 2 was finished, flanges were attached to the upstream end to allow it to be connected to one of the transitions, shown below in Figure 16. Two of the flanges are approximately 59.2 cm (23.3 in.) by 2.5 cm (1 in.), while the other two are 53.1 cm (20.9 in.) by 2.5 cm (1 in.). 3M, stage 3 Bondo body filler was used to smooth the upstream end after attaching the flanges to ensure a smooth fit between the transition and diffuser. B-shaped weather stripping was also attached to the diffuser to further seal the connection between it and the transition. During installation of diffuser 2, a rubber strip was added between the Unistrut frame built to support the wind tunnel and the diffuser to dampen vibrations. Figure 17 shows the completed diffuser construction.

Figure 16. Image of the flanges used to connect diffuser 2 with a transition piece.

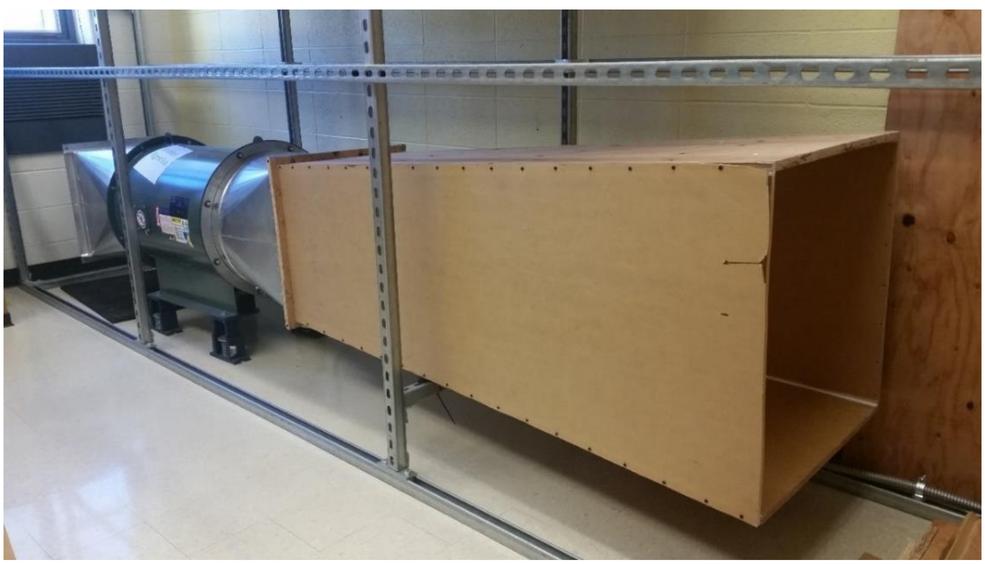

Figure 17. Image showing the second diffuser attached to the fan. The plexiglass in the front is covered by a protective layer of paper. The flanges are visible on the left end, as well as the caulk used to seal the inner edges (on the right).

4.2.2. Building Corners 1 & 2

Construction of corners 1 and 2 is still ongoing, but the design and construction considerations will be covered in this section. Each part is referred to using a similar convention to diffuser 2. The corners are shown in Figure 18. The dimensions of each part are given in Table 2.

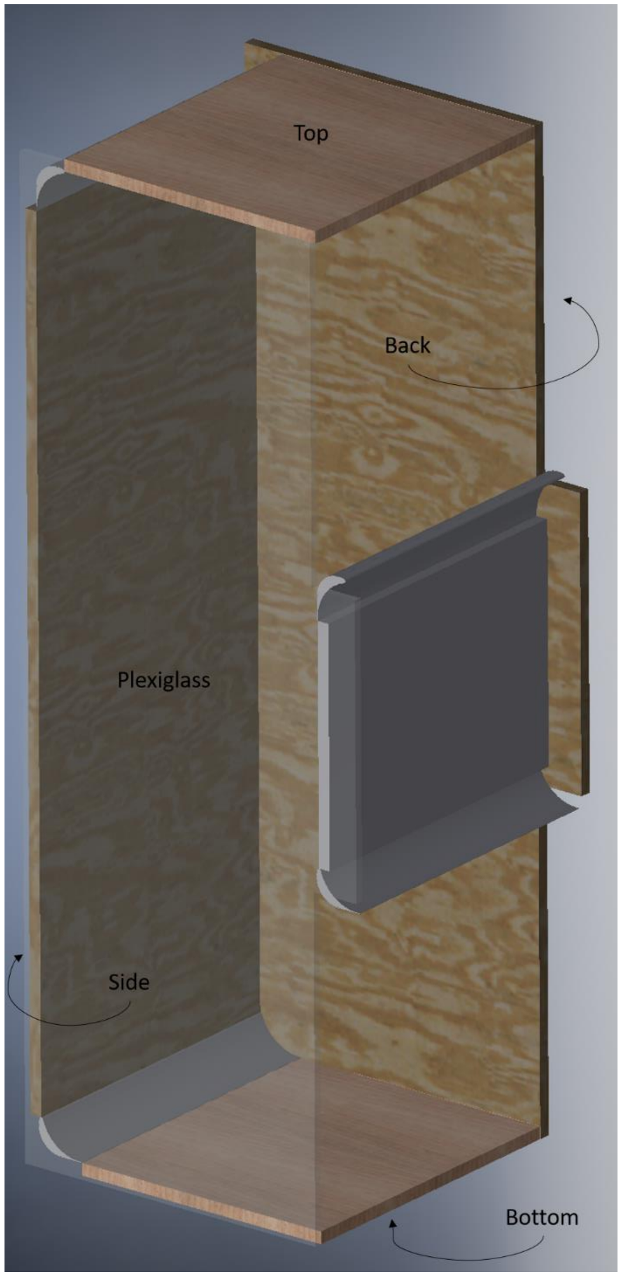

Figure 18. Image depicting corners 1 and 2, labeled.

Table 2. List of dimensions of the pieces in the corners 1 & 2 assembly.

Part Name	Width (cm)	Height (cm)
Top	44.4	49.5
Bottom	42.3	49.5
Plexiglass	51.4	152.2
Back	51.4	152.2
Side	49.5	136.2

Corners 1 and 2 are assembled as one part, to allow for simpler construction. To attach the turning vanes, it was decided that the vanes would be built inside a cascade, meaning each vane will be sandwiched between and connected to two pieces of 0.3 cm (1/8 in.) thick acrylic. Channels will be milled into the front and back sides of the corner, allowing the cascades to slide into place. An example of this cascade is illustrated in Figure 19.

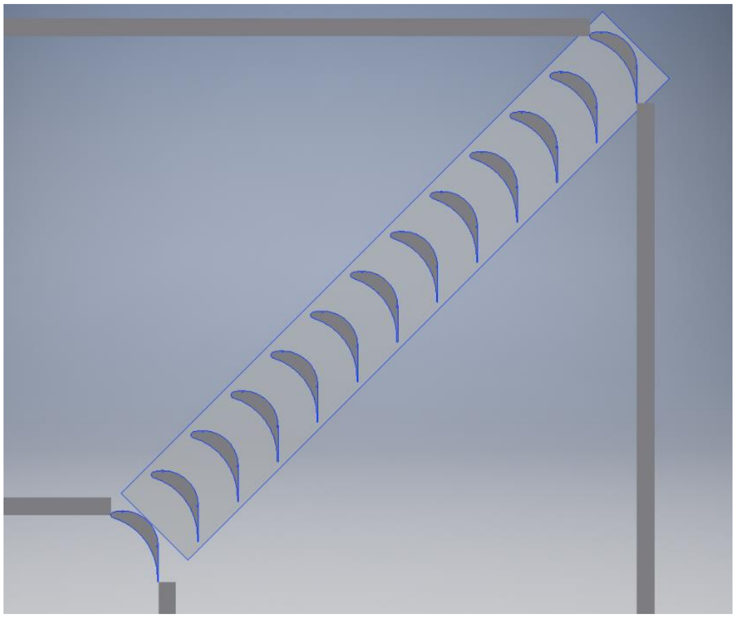

Figure 19. Illustration of what a vane cascade would look like. The cascade and vanes are highlighted.

Currently, construction of the corners is incomplete. Figure 20 shows the current progress. The sides are cut and assembled, but the front and back sides will have to be milled, and construction of the cascade has not begun.

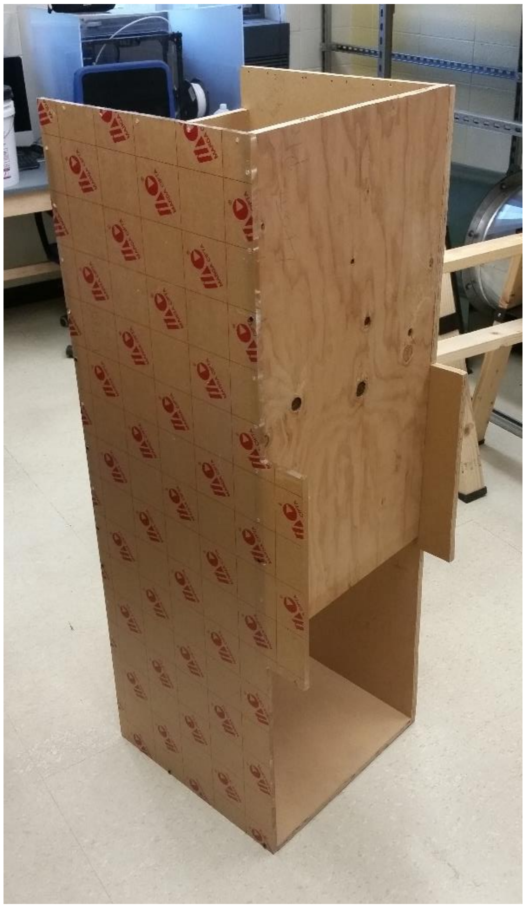

Figure 20. Picture of the current progress in constructing corners 1 and 2.

Chapter 5

CONCLUSIONS AND FUTURE WORK

5.1. Conclusions

The purpose of this work was to refine initial designs and begin construction of the Houghton College wind tunnel. This is a small-scale, low-speed, closed-return wind tunnel. The goal is to use the wind tunnel to further education and perform new research. The initial design of the wind tunnel was described, as were the most recent design refinements. Construction of one diffuser is now complete, and it is partially complete for two of the corners. Some design refinements that were necessary included shortening the two diffusers and adding the turning vane geometry to the tunnel model. One diffuser had to be shortened because the settling chamber had to be made longer, while the other had to be shortened due to an intersection with a turning vane and a transition piece. The first diffuser had to be shortened from 192.4 cm to a length of 180 cm, while the second one was shortened from 180.9 cm to 173.5 cm. Work done by Blevins confirmed that both diffusers can be shortened without experiencing flow separation [16]. Construction has finished for one diffuser and two corners, although neither of the constructed corners has been fitted with turning vanes yet.

5.2. Future Work

There is still more research to be done before the wind tunnel can be considered operational. First, more components must be constructed: corners 3 and 4, the settling chamber, the nozzle, the test section, and the first diffuser. Second, more research must be done on how measurements will be performed. One method that has been considered is using a Magnetic Suspension and Balance System (MSBS), such as the one illustrated in Figure 21. This would allow measurements of forces and moments on the test object. Forces on the object would be measured as changes in the current through the electromagnets that are levitating the object. Major difficulty comes from developing a control algorithm to keep the object centered and relating the electric currents to forces on the test object. Measuring other parameters such as fluid pressure and velocity require other instruments such as barometers and pitot-static tubes.

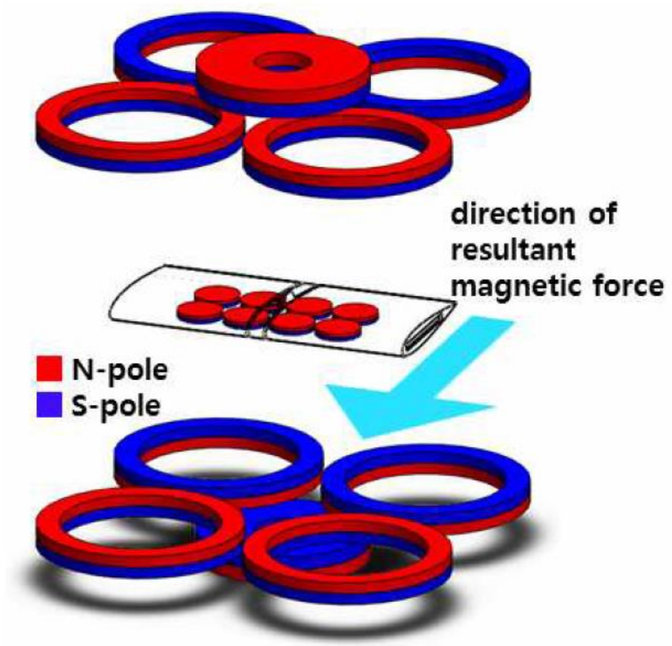

Figure 21. Diagram of a magnetic suspension and balance system. An airfoil implanted with permanent magnets is suspended using two arrays of electro-magnets and permanent magnets. The electromagnets must be actively controlled to maintain levitation of the test object. Using this system, forces on the airfoil (or any object) can be measured because they are functions of the current supplied to the electromagnets. Figure taken from Ref. [26].

Once the wind tunnel is complete, it can be used to conduct research on a variety of topics. These include classroom-based research projects or collaborative research projects with researchers outside of Houghton College. Undergraduate physics and engineering students would benefit greatly from having an operational wind tunnel on campus, allowing them to learn more about fluid dynamics experimentation. An example of a research project students might conduct is the study of how ice accumulation on wings impacts lift and drag. To make this possible, 3D scans of wings covered in ice could be obtained from an external source (e.g. NASA), 3D printed, then used in the wind tunnel for various experiments [27]. Students could also conduct research on a project of their choice, such as the lift and drag forces on 3D models of various cars or airfoils.

R e f e r e n c e s

[1] D. D. Baals and W. R. Corliss, *Wind Tunnels of NASA.* (U.S. Government Printing Office, Washington, D.C., 1981).

[2] Sir G. Cayley, The Journal of the Royal Aeronautical Society **37**, 547 (1933).

[3] F. H. Wenham, in *Seventh Annual Report of the Aeronautical Society of Great Britain for the Year 1872*. (Peter Murray Hill Ltd., London, 1956), pp. 6-12.

[4] L. P. Chamorro and F. Porté-Agel, Energies **4**, 1916-1936 (2011).

[5] C. Chang and R. N. Meroney, J. Wind Eng. And Industrial Aerodynamics **91**, 1141-1154 (2003).

[6] A. B. Bailey and J. Hiatt, AEDC Report No. TR 70-291, 1971.

[7] G. B. Cosentino, NASA Report No. TM-214636, 2008.

[8] J. D. Tannehill, D. A. Anderson, and R. H. Pletcher, *Computational Fluid Mechanics and Heat Transfer,* 2nd ed. (Taylor & Francis, Philadelphia, 1997).

[9] J. D. Jaramillo, B.S. Thesis, Houghton College, 2017.

[10] D. J. Eager, B.S. Thesis, Houghton College, 2018.

[11] J. S. Martin, B.S. Thesis, Houghton College, 2019.

[12] I. G. Currie, *Fundamental Mechanics of Fluids,* 3rd ed. (Taylor & Francis, Boca Raton, 2003).

[13] J. D. Anderson Jr. *Fundamentals of Aerodynamics*, 4th ed. (McGraw-Hill, New York City, 2004).

[14] J.B. Barlow, W. H. Rae Jr., and A. Pope, *Low-Speed Wind Tunnel Testing,* 3rd ed. (John Wiley & Sons, New York City, 1999).

[15] P. Bradshaw and R. C. Pankhurst, Prog. Aeronaut Sci. **5**, 1-59 (1964).

[16] R. D. Blevins, *Applied Fluid Dynamics Handbook*. (Van Nostrand Reinhold Co., New York, 1984).

[17] W. T. Eckert, K. W. Mort and J. Jope, NASA Report No. TN D-8243, 1976.

[18] G. Krober, NACA TM 722, 1932.

[19] G. Klein, K. Tupper, and J. Green, Canadian Journal of Research **3**, 272-285 (1930).

[20] J. H. Bell and R. D. Mehta, NASA CR 177488 (1988).

[21] D. Brassard, J. Fluids Eng. **127**, 183-185 (2005).

[22] T. Morel, J. Fluids Eng. **97**, 225-233 (1975).

[23] R. W. Fox and S. J. Kline, S. Basic Eng. **84**, 303-316 (1972).

[24] A. T. McDonald, R. W. Fox, Int. J. Mech. Sci., **8**, 125-139 (1966).

[25] J. H. G. Howard, et al., ASME Paper 67-WA/FE-21, 1967.

[26] D. K. Lee, J. S. Lee, J. H. Han, and Y. Kawamura, J. Mech. Sci. and Tech. **27**, 1963-1970 (2013).

[27] S. Lee, A. P. Broeren, H. E. Addy, R. Sills, E. M. Pifer, NASA Report No. TM-217702, 2012.